Experimental Investigation of Particle Pinch Associated with Turbulence in LHD Heliotron and JT-60U Tokamak Plasmas

K. Tanaka 1), H. Takenaga 2), K. Muraoka 3), C. Michael 4), L. N. Vyacheslavov 5), M. Yokoyama 1), H. Yamada 1), N. Oyama 2), H. Urano 2), Y. Kamada 2), S. Murakami 6), A. Wakasa 7), T. Tokuzawa 1), T. Akiyama 1), K. Kawahata 1), M. Yoshinuma1), K. Ida 1), I. Yamada 1), K. Narihara 1), N. Tamura 1) and the LHD experimental group 1)

1)National Institute for Fusion Science, Toki 509-5292, Japan
2)Japan Atomic Energy Agency, 801-1 Mukouyama, Naka, Ibaraki 311-0193, Japan
3)Chubu University, 1200 Matsumoto, Kasugai, Aichi 487-8501, Japan
4) EURATOM/UAKEA Fusion Association, Oxfordshire OX14 3 DB, United Kingdom
5) Budker Institute of Nuclear Physics, 630090, Novosibirsk, Russia
6) Department of Nuclear Engineering, Kyoto University, Kyoto 606-8501, Japan
7) Graduate School of Engineering, Sapporo Hokkaido University, 060-8628, Japan

e-mail contact of main author: ktanaka@LHD.nifs.ac.jp

Abstract. Comparative studies were carried out to elucidate the most essential parameter(s) for control of density profiles in LHD heliotron and JT-60U tokamak plasmas. Different collisionality dependence was found between two devices. Change of fluctuation property was observed at different density profile in both devices in plasma core region. In JT-60U, increase of radial correlation length was observed at higher power of neutral beam heating (P_{NB}) with increase of density peaking. In magnetic axis positions (R_{ax}) at 3.6m of LHD, the peak wavenumber did not change at higher P_{NB} with decrease of density peaking. The simple mixing length estimation shows larger contribution of turbulence driven transport in JT-60U compared with R_{ax}=3.6m of LHD.

1. Introduction

Understanding of physics mechanism of electron density profile formation is one of the essential issues for control of future fusion reactor in both heliotron/stellarator and tokamak devices. Many experimental works and theoretical investigations suggest the role of neoclassical effects and turbulence. The neoclassical mechanism is driven by the collisions of confined particles and described by well developed theoretical model. The main contributors to the turbulence mechanism are the ion temperature gradient mode (ITG) and the trapped electron mode (TEM). Neoclassical mechanism can account for experimentally observed profiles in both devices in the limited operation regimes. However, in many other regimes,this mechanism is too weak to be responsible for observed density profiles. Many theoretical models of anomalous particle transport were proposed still, none of them can explain a number of experimental observations. In addition, the role of turbulence in building density profiles is not clear experimentally because measurements in plasma core region are very limited. Therefore, it is essential to continue studying relation between turbulence and density profile.

2. General comparison of density profiles between JT60-U and LHD

Figure 1 shows radial profiles of electron density (n_e) and electron temperature (T_e) of JT-60U and LHD with neutral beam (NB) heating. Clear differences of density profiles can be seen for the different densities in JT-60U and for the different R_{ax} in LHD. Particle sources from walls decreased exponentially and did not affect the core density profiles (at ρ<1.0) in both

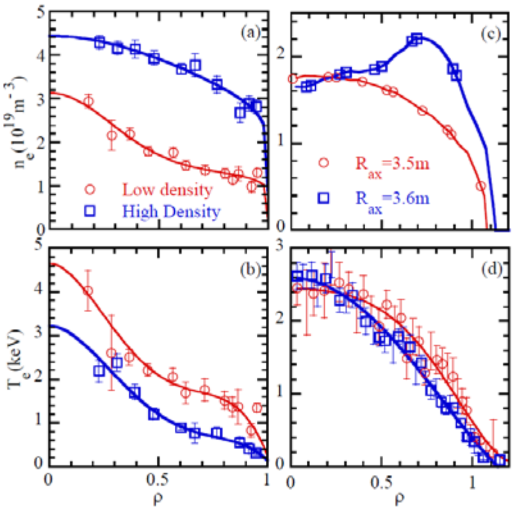

Fig. 1 (a), (c) n_e, and (b),(d) T_e profiles. (a) and (b) from JT-60U, and (c) and (d) from LHD. Here, plasmas in low and high density plasmas in JT-60U, and those at R_{ax}=3.5m and R_{ax}=3.6m in LHD are compared.

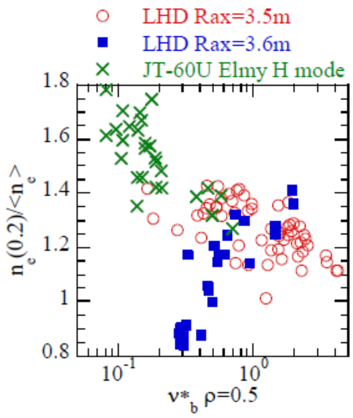

*Fig.2 Dependence of the density peaking factor on ν_b**

devices. In JT-60U, the central particle source was changed by a factor three by the combination of NB and electron cyclotron heating powers. However, the density peaking factor did not change [1]. In LHD, central particle fueling increased by a factor eight with an increase of NB powers at R_{ax}=3.6 m, resulting in the changes density profiles from peaked to hollow although NB fueling supplied particles more to the core than to the edge [2] Carbon impurity profiles did not change in both devices, indicating that impurity accumulation did not affect density profiles. These suggest the changes of density profiles to be not due to the difference of particle fueling, but due to the difference of transport in both devices. In JT-60U, the contribution of the neoclassical Ware pinch was negligible, thus requiring to invoke an anomalous inwardly directed pinch. As shown in Figs. 1 (a) and (b), the density profile in JT-60U is more peaked at a low value of n_e and/or a high value of T_e. This fact may indicate an anomalous inward pinch being larger with decreasing collisionality. In LHD, neoclassical transport is minimized by reducing the effective helical ripple at around R_{ax}=3.5-3.6 m [3] and has almost the same value for both positions. Therefore, the observed difference of density profiles is due to different contribution of anomalous transport for R_{ax} = 3.5 m and 3.6 m.

Figure 2 shows the dependence of density peaking factors on an electron-ion collision frequency normalized by the trapped electron bounce frequency (ν^*_b). The density peaking factor was defined as the ratio of the density at ρ=0.2 against the volume averaged density and ν^*_b was estimated at ρ=0.5. As shown in Fig. 2, density peaking factors increased with decreasing ν^*_b in JT-60U. The origin of density peaking in tokamaks is theoretically suggested as due to the turbulence-driven inward pinch, resulting in the increase of the density peaking factor with decreasing collisionality [4]. In LHD at R_{ax}=3.5 m, density peaking factors moderately increased with decreasing ν^*_b as well and only peaked density profiles were observed. On the other hand, a different ν^*_b dependence was observed at 3.6 m where density peaking factors decreased with decreasing ν^*_b. Particle convection velocities for R_{ax}=3.6 m, which were estimated using a density-modulation experiment [2], were outwardly directed and close to neoclassical values at lower collisionality, suggesting that particle transport (thus the observed ν^*_b dependence shown in Fig. 2) was affected by neoclassical processes.

3. Response of turbulence under change of density profiles in JT-60U

Density profile in JT-60U becomes peaked one at lower collisionality as shown in Fig.2. Thus increase of NB power with constant external fueling induce density peaking. Figure 3 and 4 shows such examples in the Elmy H mode discharge similar to the data set of Fig.2. The neutral beam power increases from 7.4 to 12.9MW in time as shown in Fig.3. (a), then, density profile becames slightly peaked as shown in Fig.4 Central line integrated density increases with increase of NB power as shown in Fig.3 (b), however, the increase of beam source is not dominant effect as mentioned in the previous section.

The characteristic of turbulence was measured by O mode correlation reflectometer [5] employing two close frequencies. One is fixed at 47.3GHz while the other is scanned 42.3-46.8GHz in 6 step in time. Each step is 20ms, then cross correlation of the reflected power was measured in 120msec for the density regimes 2.23-2.78x10^{19}m^{-3}. The radial correlation length (l_c) was estimated from radial profile of the coherence like in Fig.5. For the quantitative estimation of l_c, the radial correlation profile was determined from the exponential fitting function.

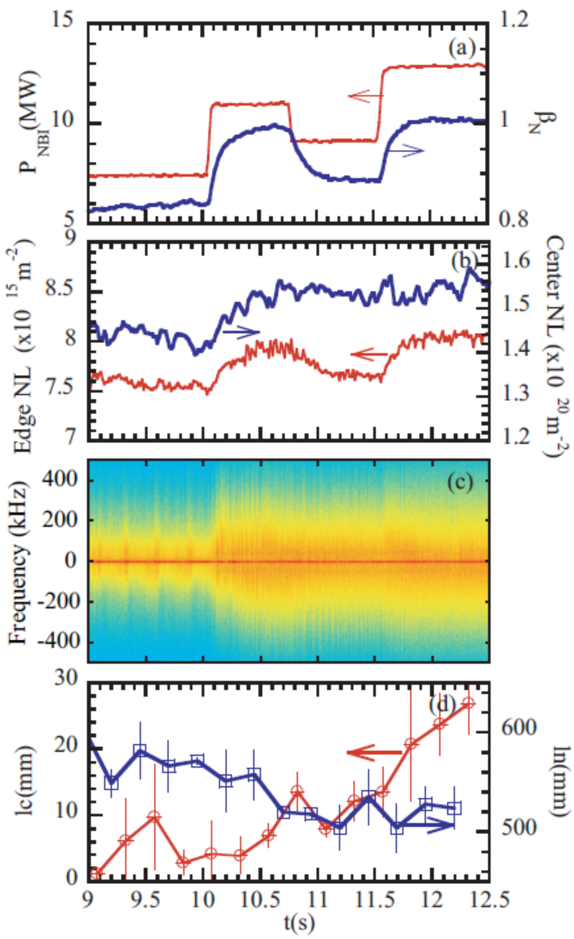

Fig.3 Time history of (a) NB power, nolmalized beta (β_n), (b) line integrated density (c)reflected power spectrum and (d)density scale length, radial correlation length in JT-60U.

Figure 3 (c) shows time history of power spectrum of fixed frequency channel. Frequency spectrum becomes broad after t=10s, when NB power increased suggesting change of turbulence characteristics. In addition, l_c changed drastically with increase of P_{NB}. Clear difference was observed between low and high P_{NB} as shown in Fig.5. Radial correlation increased with increase of heating power. The change of density scale length $l_n=(1/n_e\ dn_e/dr)^{-1}$ around cut off position of reflectometer was estimated from two channels of YAG Thomson scattering, which were at ρ-0.15 and 0.5. As shown in Fig.3 (d), radial correlation length (l_c) increased with decrease of density scale length. Figure 6 shows relation between l_n and l_c. Although change of density scale length in Fig.3 and 4 were modest, clear relation between l_n and l_c was found. The radial correlation length became longer with decrease of l_n. This suggests longer l_c induces higher density peaking.

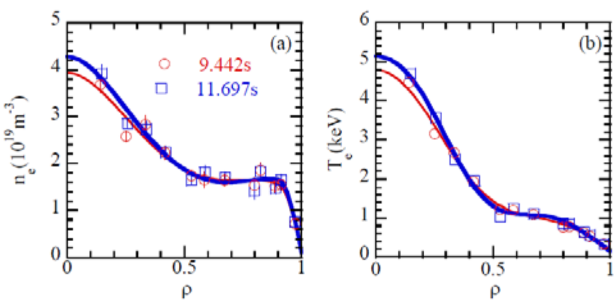

Fig.4 (a) n_e and (b) T_e profile at high (7.4MW, t=9.442s) and low (12.8MW, t=11.697s)NB power

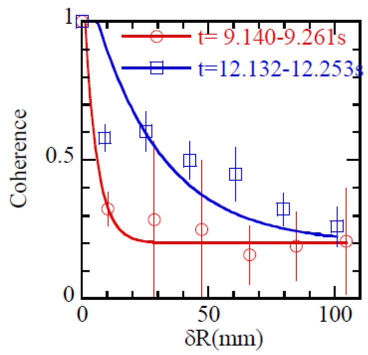

Fig5 Radial coherence at ρ-0.3

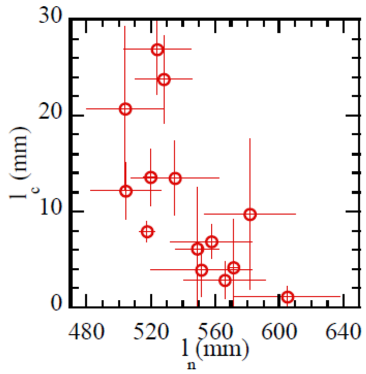

Fig.6 Relation between l_n and l_c

4. Response of turbulence under change of density profiles in LHD

Change of density profile under temporal scan of P_{NB} is also observed in LHD. Figure 7 shows temporal behavior of density, temperature and fluctuation behavior. The fluctuation was measured by the two-dimensional phase contrast imaging (2D-PCI)[6]. The measured wavenumber components are poloidally dominated. As shown in Fig.7 (a) and (b), electron density decrease when NB power increases after t=4.1sec. This is opposite response to the one observed in JT-60U. However, it should be noted that there are two important differences between observations in JT-60U and LHD. One is difference of magnetic configuration. As described in Sec.2, collisonality dependence of density peaking factor depends on magnetic configuration. The second difference is power deposition of NBI into plasma components. For the data set of this article in LHD NBI heat predominantly electrons, while in JT-60U main NBI power deposits mainly into ions. The electron heating in LHD is due to the high acceleration voltage (-160keV) of negative ion based neutral beam (N-NB). Especially, when density is low (line averaged density is less than -2x$10^{19}$$m^{-3}$), electron temperature is usually higher than ion temperature. As shown in Fig.7 (c), $T_e(0)/T_i(0)$ increases after t=4.1sec with increase of P_{NB}. In tokamak gyro-kinetic theory, increase of T_e/T_i can cause density

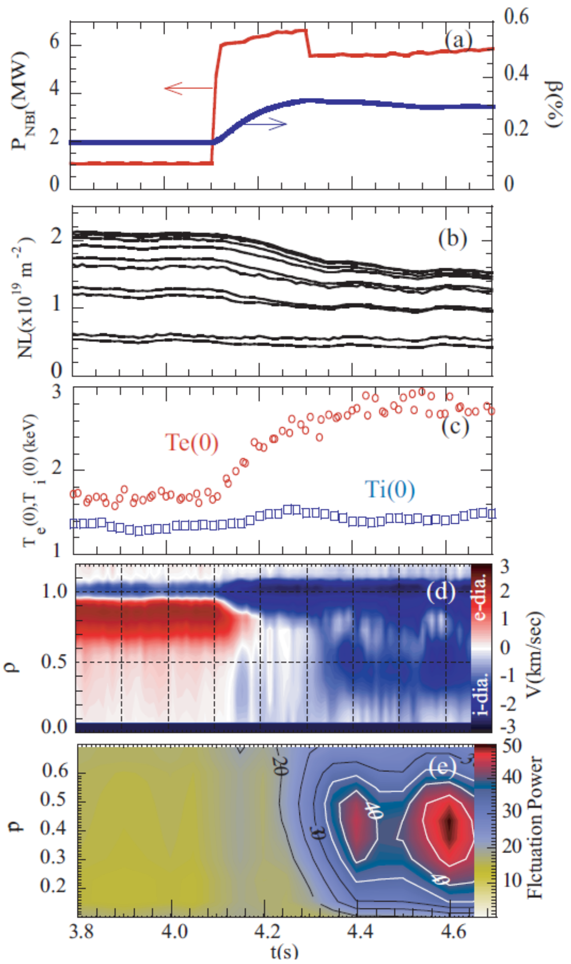

Fig.7 Time history of (a) NB heating power, diamagnetic β, (b) line integrated denity. Higher values (upper trance)corresponds to the chord close to magnetic axis. (c) central electron and ion temperature, (d) fluctuation phase velocity and (e) fluctuation power at ρ=0-0.7. R_{ax}=3.6m, Bt=2.75T. In Fig.7(d), red and blue colors indicate electron and ion diamagnetic direction in labolatory frame respectively.

flattening due to increase of thermo-diffusion, and fluctuation shifts from ITG to TEM. This theoretical prediction qualitatively account for density flattening caused by electron cyclotron heating (ECRH) [7]. Density flattening observed in LHD is similar to ECRH heating in tokamaks.

As shown in Fig. 7 (d) and (e), fluctuation properties changed with reduction of density. Measured wavenumber was poloidally dominated, thus, poloidal phase velocity in laboratory frame was measured. As shown in Fig 7 (e), phase velocity inside last closed flux surface was directed to the electron diamagnetic (e-dia.) direction before increase of NB power then switch to the ion diamagnetic (i-dia.) direction after increase of P_{NB}. As shown in Fig. 7 (e), core (ρ=0.-0.7) fluctuation power increased after increase of P_{NB}.

Figure 8 shows radial profile of radial electric field (E_r), diffusion coefficient (D), convection velocity (V), n_e, T_e profiles and fluctuation profiles at low (1.1MW, at t=4.0s) and high (5.6MW, at t=4.5s) NB power. The experimental values of D and V were estimated from density modulation experiments in this discharge. The radial electric fields were estimated from neoclassical ambipolar condition. The neoclassical values (E_r, D and V) were estimated from GSRAKE code [8]. In Fig.8 (g), (h), (i), three different neoclassical values are shown at ρ>0.5. These are possible three roots of neoclassical ambipolar condition.

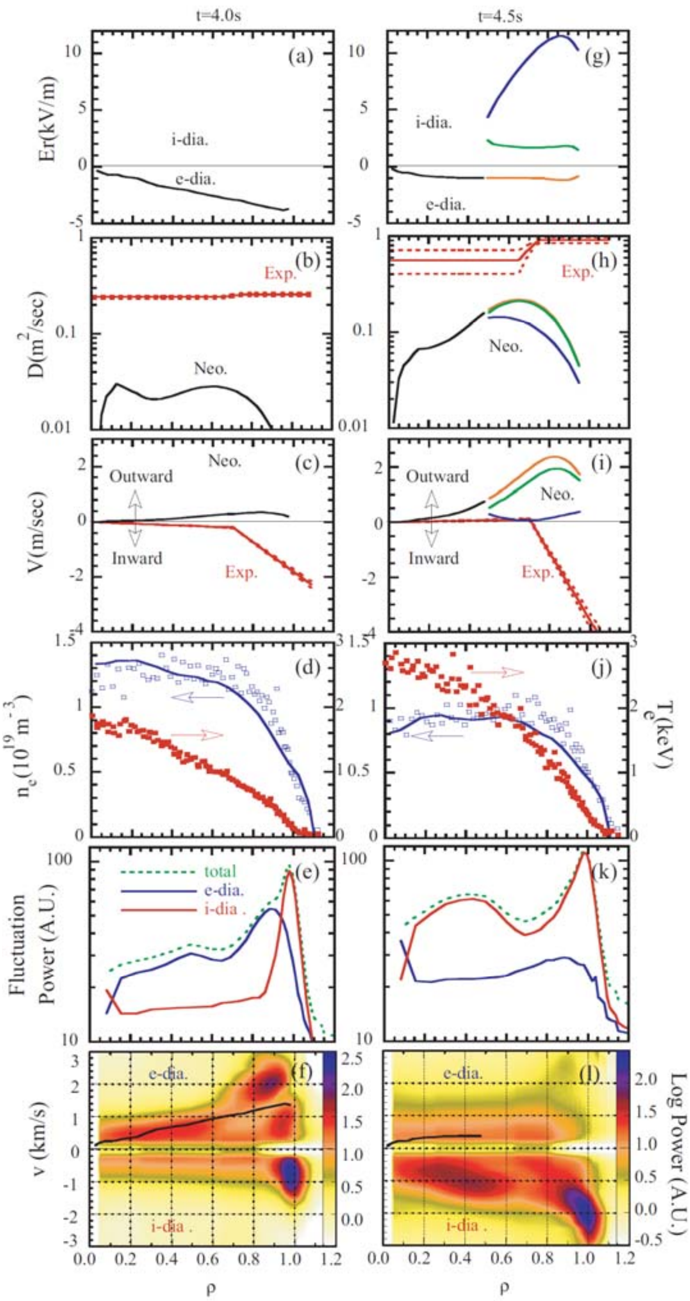

Fig.8(a), (g) Radial profile of E_r, (b), (h) D, (c),(i) V, (d),(j) n_e T_e, (e), (k) fluctuation power and (f), (l) fluctaution phase velocity. (a)-(f) are at low NB power (1.1MW at t=4.0s) and (g)-(l) are at high NB power (5.6MW at t=4.5s). Neoclassical E_rxB_t roation velocities are indicated by black lines in Fig.8 (f) and (l).

As shown in Fig.8 (d) and (j), the n_e profiles changed from peaked one to slightly hollow one. Especially reduction of density is very drastic at ρ < 0.7. The electron temperature increased around factor 1.5, however, temperature scale length, which is $l_t=(1/T_e\ dT_e/dr)^{-1}$, is almost constant. This is mainly due to the broad deposition of NB heating. It cannot be concluded from this data set if T_e profile in LHD is stiff like in tokamak. The change of density profile, which is from peaked to hollow, is caused by the increase of outward convection. The outward convection is likely due to outward diffusion, however, increase of thermo diffusion is not due to the reduction of l_t (since it is almost constant) but due to the change of T_e itself [9, 10]. The experimental diffusion coefficients are larger than neoclassical values in whole region as shown in Fig.8 (b) and (h), although the difference of experimental D became closer to the neoclassical D at t=4.5s with higher P_{NB}. The inward directed pinch was observed at t=4s of low NB heating and this becomes outward at t=4.5s with higher P_{NB}. The neoclassical V indicates outward at both case. As described in Sec.II, neoclassical effect can play role on density profile at R_{ax}=3.6m, which is same configuration of data in Fig. 7 and 8. Especially convection velocity in core region ρ<0.7 is comparable with neoclassical estimation and its T_e dependence is similar in experimental and neoclassical values at R_{ax}=3.6m [10].

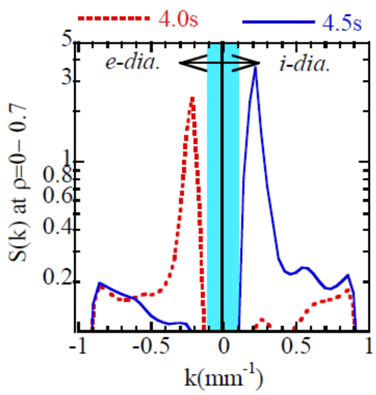

Fig.9 Wavenumber spectrum at ρ=0-0.7. Colored region -1<k<1mm^{-1} is instrumental cut off region

As shown in Fig.8 (e) and (k), strongest fluctuation power existed at around ρ=1.0. This is similar observations to toroidal devices. But another peaks were observed at around ρ=0.4 at both timing. As shown in Fig.7 (d),(e) and Fig.8 (e), (k), fluctuation power in core region increased with increase of NB power, increase of T_e/T_i and decrease of density. In addition fluctuation phase velocity changed from e-dia. to i-dia. direction in laboratory frame. The neoclassical $E_r xB_t$ rotation velocity was shown in Fig.8 (f) and (l). According to neoclassical estimation, poloidal rotation is directed to the e-dia. direction both at t=4.0 in ρ<1.0 and at t=4.5s in ρ<0.5. Thus change of observed phase velocity from e-dia. to i-dia. direction at ρ<0.5 can be due to change of phase velocity of fluctuation itself. Excluding $E_r xB_t$ rotation, fluctuation phase velocity in plasma frame became almost zero at t=4.0s and turned to i-dia. direction at t=4.5s. Tokamak gyro-kinetic linear calculation shows switch from ITG to TEM with increase of T_e/T_i, which corresponds to change from i-dia, to e-dia. direction [7]. This does not agree with observations in LHD.

Figure 9 shows comparison of wavenumber spectrum in the core region (ρ=0-0.7), where density reduction was observed. The absolute value of the peak wavenuber is almost same (-0.2mm^{-1}) with low and high P_{NB}, although propagation direction switched.

5. Discussion and Summary

The particle flux Γ is written as follows:

$$\Gamma = -D\nabla n_e + n_e V \tag{1}$$

In plasma core region, particle source can be negligible in both devices as described in Sec. II, then, in steady state particle flux can be zero. Then we obtain the following equation.

$$\frac{\nabla n_e}{n_e} = \frac{V}{D} \tag{2}$$

The mixing length theory tells diffusion coefficient of turbulent media is proportional to mutli product of correlation length l_c and background flow velocity v_d. In magnetized plasma,

v_d is drift velocity and l_c is plasma minor radius for Bohm diffusion and l_c is ion Larmor radius for Gyro Bhom diffusion [11]. Then, the turbulent driven diffusion coefficient was estimated as follows.

$$D = \alpha\, l_c\, V_d = \alpha\, l_c\, \frac{\nabla P_e}{e n_e B_t} = \alpha\, l_c\, \frac{k_B T_e}{e B_t}\left(\frac{1}{n_e}\frac{dn_e}{dr} + \frac{1}{T_e}\frac{dT_e}{dr}\right) \qquad (3)$$

Here, α was set to be 1/16, which is Bohm factor. In JT-60U, l_c was experimentally estimated from reflectometry measurements as described in Sec. 3. In LHD, l_c was estimated by $l_c=2\pi/k$, where k is measured peak wavenumber by using 2D-PCI. The measured k by the 2D PCI was dominated by poloidal components rather than radial components. The correlation length should be radial one in eq.(3), thus, the estimation of l_c in LHD assumed that wavenumber spectrum is isotropic in radial and ploidal direction. Then, the convection velocity was estimated from eq.(2) using D from eq.(3). These indicate rough estimation of turbulence driven diffusion coefficient and convection velocity.

The comparisons of turbulence driven D and V were done in the core region, where density profile changed under scanning P_{NB} in both devices. In JT60-U, normalized T_e and n_e gradients were estimated from two measurements point of YAG Thomson scattering at ρ=0.15 and 0.5 as described in Sec. 3. In LHD, normalized T_e and n_e gradients are estimated at ρ=0.4 from the profiles in Fig.8 (d) and (j). The peak wavenumber from Fig.9 was used for the estimation of l_c.

Table 1 shows summary of comparison of P_{NB}. Table2 shows summary of comparison of turbulence driven D and V. Table 3 shows comparison of D and V in LHD from density modulation experiments and neoclassical estimation. The diffusion coefficients and convection velocities from density modulation experiments indicate the transport coefficients for total transport, which are sum of anomalous and neoclassical transport.

In JT-60U, both turbulence induced D and V increased with increase of heating power and V increases larger than D. The increase of D at higher P_{NB} is mainly due to the increase of l_c. The convection velocity increased higher than D. This is due to the larger V_d at higher P_{NB}. It is reasonable that D becomes higher with higher P_{NB} due to the power degradation effect. Higher increase of V than D with higher P_{NB} induced more peaked density profile.

On the other hands, in LHD both turbulence driven D and V decreased with increase of the P_{NB} as shown in table 2. The decrease of turbulence driven D at higher P_{NB} is due to constant peak wavenumber and reduction of V_d. The reduction of V_d is mainly due to the reduction of normalized n_e gradient. It is clear contrast that D for total transport increased at higher P_{NB} as shown in table.3. Core density reduced clearly, so, reduction of trubulence driven D does not account for experimental observation. The contribution of neoclassical D increases at higher P_{NB} as shown inFig.8 (b) and (h). One of the possible interpretation is increase of D for total transport is mainly due to the increase of neoclassical diffusion. However, still D for total transport at higher P_{NB} is around factor five larger than neoclassical values at ρ=0.4.

From the previous results in LHD, the convection for total transport was comparable with neoclassical one. With higher P_{NB} reduce core density and collsionality becomes smaller, then, convection for total transport becomes closer to neoclassical values [2,10]. The fluctuation power in core region (ρ=0-0.7) increased with increase of P_{NB} as shown in Fig.8 (e), (k) and Fig.9, however according to simple mixing model given by eq. (3), the turbulence does not contribute significantly in core region. This might be the reason of difference of collisonality dependence of the density peaking factor at R_{ax}=3.6m of LHD and that of JT-60U. Change of the fluctuation property is more moderate in LHD compared with JT-60U, although P_{NB} scanned more drastically in LHD. This indicates role of turbulence is stronger in tokamak more than in helical device.

Since mixing length estimation is too simplified, detail comparison with linear and non linear modeling and experimental survey in wider region (different collisionality, different configuration including R_{ax}=3.5m of LHD) are required for further understanding. Especially saturated fluctuation power should be considered. Quasi-linear estimation will be useful for this consideration. Also the observed difference of fluctuation property and density response partly might be due to the difference of ion heating in JT-60U and electron heating in LHD. The effect of heating deposition should be considered as well.

	$P_{NB\ low}$(MW)	$P_{NB\ high}$(MW)	P_{NBhigh}/P_{NBlow}
JT-60U	7.4	12.8	1.7
LHD	1.1	5.6	5.1

Table 1. Comparison of P_{NB}

	$D_{low\ power}$ (m^2/s)	$D_{high\ power}$ (m^2/s)	$D_{high\ power}/D_{low\ power}$	$V_{low\ power}$ (m/s)	$V_{high\ power}$ (m/s)	$V_{high\ power}/V_{low\ power}$
JT-60U	2.5	6.0	2.4	-4.2	-12.0	2.9
LHD	1.7	1.1	0.6	-0.7	0.2	-0.3

Table 2 Comparison of turbulence driven D and V

	$D_{low\ power}$ (m^2/s)	$D_{high\ power}$ (m^2/s)	$D_{high\ power}/D_{low\ power}$	$V_{low\ power}$ (m/s)	$V_{high\ power}$ (m/s)	$V_{high\ power}/V_{low\ power}$
LHD_{total}	0.24	0.56	2.3	-0.12	0.06	-0.5
$LHD_{Neo.}$	0.02	0.12	6.0	0.12	0.49	4.1

Table 3 Comparison of D and V in LHD from density modulation experiments at ρ=0.4. D and V are values for total transport and neoclassical estimation

References

[1] TAKENAGA, H., et al., 2008 Nucl. Fusion **48** 075004
[2] TANAKA KA, K., et al., 2007 Fusion Sci. Tech **51** 97
[3] MURAKAMI, S., et al., 2002 Nucl. Fusion **42** L19
[4] ANGIONI, C., et al., 2003 Phys. Plasmas **10** 3225
[5] OYAMA, N., *in preparation*
[6] TANAKA, K., et al., Rev. Sci. Instrum. in press
[7] ANGIONI, C., et al., 2004 Nucl. Fusion 44 827
[8] BEIDLER, C. D., et al., 1995 Plasma Phys. Control. Fusion, **37**, 463
[9] TANAKA, K., 2008 Nucl. Fusion 039801
[10] TANAKA, K., 2008 Plasma Fusion Res. 3, S1069
[11] KADOMTSEV, B,B., “Tokamak Plasma: A Complex Physical System”, IOP publishing Ltd 1992